

A Numerical Model of Skin Electroporation Based on *In Vivo* Experiments

NATAŠA PAVŠELJ,¹ VERONIQUE PRÉAT,² and DAMIJAN MIKLAVČIČ¹

¹Faculty of Electrical Engineering, University of Ljubljana, Tržaška 25, SI-1000 Ljubljana, Slovenia; and ²Department of Pharmaceutical Technology, Université Catholique de Louvain, 1200 Brussels, Belgium

(Received 18 April 2007; accepted 24 August 2007; published online 12 September 2007)

Abstract—As an alternative to viral methods that are controversial because of their safety issues, chemical and physical methods have been developed to enhance gene expression in tissues. Reversible increase of the cell membrane permeability caused by the electric field—electroporation—is currently one of the most efficient and simple non-viral methods of gene transfer. We performed a series of *in vivo* experiments, delivering plasmids to rat skin using external plate electrodes. The experiments showed that skin layers below stratum corneum can be permeabilized in this way. In order to study the course of skin tissue permeabilization by means of electric pulses, a numerical model using the finite element method was made. The model is based on the tissue-electrode geometry and electric pulses used in our *in vivo* experiments. We took into account the layered structure of skin and changes of its bulk electrical properties during electroporation, as observed in the *in vivo* experiments. We were using tissue conductivity values found in literature and experimentally determined electric field threshold values needed for tissue permeabilization. The results obtained with the model are in good agreement with the *in vivo* results of gene transfection in rat skin. With the model presented we used the available data to explain the mechanism of the tissue electroporation propagation beyond the initial conditions dictated by the tissue initial conductivities, thus contributing to a more in-depth understanding of this process. Such a model can be used to optimize and develop electrodes and pulse parameters.

Keywords—Electroporation, Electro gene transfer, Finite element method, Plate electrodes.

INTRODUCTION

Skin covers the entire external surface of human body, is the principal site of interaction with the surrounding world and a protective barrier preventing internal tissues from exposure to trauma, ultraviolet

radiation, temperature extremes, toxins, and bacteria.⁹ Due to its size and accessibility, skin is an attractive target tissue for a variety of applications, *in vivo* gene delivery being one of them. It can be used in treatment of skin disorders or for systemic effect to treat diseases of other organs. Skin is also a very good target organ for DNA immunization because of the large number of potent antigen presenting cells, critical for an effective immune response.^{2,27} If necessary, large areas of skin can be treated and can easily be monitored for potential complications.

Unfortunately, the delivery of therapeutic genes to cells and tissues is still a serious bottleneck in gene therapy-based treatments since cell membrane is, in general, impermeable for larger molecules, such as drug molecules or DNA. Viral vectors, although successful in delivering therapeutic genes, pose a safety issue.³ Therefore, chemical and physical methods have been developed to enhance gene expression in cells.⁸ Reversible increase of cell membrane permeability caused by electric field—electroporation—is currently one of the most efficient and simple non-viral methods of gene transfer.^{10,19} Cell membrane is permeabilized when the threshold transmembrane voltage is reached, i.e., when the external electric field is above the threshold value. Induced transmembrane potential depends on cell and tissue parameters (tissue conductivity, cell size, shape, and distribution)^{12,20,22} and pulse parameters (pulse duration, amplitude, and number of pulses).²⁴ After treatment, cell membrane reseals provided the applied voltage was, although high enough to cause cell membrane permeabilization, still low enough not to cause irreversible permeabilization, hence permanent damage.

During our study, *in vivo* experiments were performed in order to prove the efficacy of electroporation for gene delivery in skin.¹⁴ Moreover, a numerical model was made in order to describe theoretically the process of skin electroporation. Tissue-electrode geometry, pulse parameters, and current/voltage

Address correspondence to Damijan Miklavčič, Faculty of Electrical Engineering, University of Ljubljana, Tržaška 25, SI-1000 Ljubljana, Slovenia. Electronic mail: damijan.miklavcic@fe.uni-lj.si

measurements from the *in vivo* experiments were used to develop the model.

When referring to its electrical properties, skin is a very intricate tissue due to its highly inhomogeneous structure. It consists of three main layers: epidermis (important in the immune response), dermis (gives firmness and elasticity), and subcutaneous tissue (mechanical stress absorber, thermo-insulating function). Skin epidermis is made up of different layers, but the one that defines its electrical properties the most is the outermost layer, the stratum corneum. Although very thin (typically around 20 μm), it contributes a great deal to the electrical properties of skin. Its low conductivity (three to four orders of magnitude lower than the conductivities of deeper skin layers) makes skin one of the least conductive tissues in the human body.^{1,25,26} Therefore, in applications where electric pulses are applied externally, through skin, one might expect high (too high) voltage amplitudes needed in order to breach the highly resistive stratum corneum and permeabilize viable skin layers underneath. However, as the *in vivo* experiments show, the voltages needed for skin permeabilization are in the range of those needed in other, much more electrically conductive biological tissues. One thing we observed from current and past *in vivo* experiments was the nonlinear current/voltage dependence measured during pulse delivery, suggesting tissue conductivity changes during tissue electroporation. Skin layers can be seen as serially connected resistors. Applying voltage on such a circuit (known as voltage divider) causes the voltage to be distributed between the resistors proportionally to their resistivities. Upon applying electric pulses on skin fold through external plate electrodes, almost the entire applied voltage thus rests across the highly resistive (poorly conductive) stratum corneum, which causes a very high electric field in that layer. At the same time, the electric field in deeper layers of skin—the layers targeted for gene transfection—stays too low for a successful electroporation. This fact raises the question of how is a successful electroporation-mediated DNA delivery to the dermis and the viable epidermis still possible when external plate electrodes are used. We hypothesized that the answer lies in the increase in bulk conductivities of the skin layers during electroporation, a phenomenon that was also observed *in vivo* for other tissues.^{11,13,21} This conductivity increase leads to a changed electric field distribution, which exposes the skin layers below stratum corneum to an electric field high enough for a successful permeabilization. To support this hypothesis, we described the process of skin electroporation with a numerical model, taking into account skin's layered structure and the changes of its bulk electrical properties during the electroporation.

Such a model provides a more in-depth understanding of the process of skin electroporation and will, further improved, allow predicting the outcome of pulse delivery before the treatment, thus helping in optimizing/choosing the right pulse parameters and the development of electrode geometries.

MATERIALS AND METHODS

In Vivo Experiments

To demonstrate the effectiveness of electroporation transfer and localize gene expression in transfected skin, plasmid coding for a green fluorescent protein was used (pCMVGFP). It was injected intradermally into rat skin before the application of electric pulses. The animals were anesthetized. The skin on the back was shaved 1–2 days prior to the experiments and all hair was thoroughly removed in order to allow for better visualization of plasmid injection and the area to be electroporated. For pulse delivery, we used the square-wave electropulsator Cliniporator (IGEA, Carpi, Italy). The electric pulses were delivered using two parallel, stainless-steel plate electrodes of 0.5 mm thickness and 4 mm distance (IGEA, Carpi, Italy). The area of the electrodes in contact with skin was about $1 \times 1 \text{ cm}^2$. To assure good contact between the skin fold and the electrodes, a conductive gel (EKO-GEL, ultrasound transmission gel, Egna, Italy) was applied. During the electric pulse, the actual current delivered and the applied voltage were acquired by the Cliniporator and stored on computer. Two days after the electroporation, the rats were sacrificed and the electroporated skin areas were excised. To assess the pCMVGFP expression, the epidermal and the dermal side of the samples were observed without fixation or freezing with a confocal microscope.

Numerical Calculations

Electric field and reaction current calculations were made by means of commercially available software COMSOL Multiphysics 3.3 (COMSOL, Los Angeles, CA, USA) based on finite element method. This method solves partial differential equations by dividing the model into smaller elements where the quantity to be determined is approximated with a function or is assumed to be constant throughout the element. Finite elements can be of different shapes and sizes, which allows modeling of intricate geometries. Inhomogeneities and anisotropies can also be modeled and different excitations and boundary conditions can be applied easily. The mesh of the model was set denser around the electrodes and in the thinner skin layers. As a result, the number of finite elements was very high, so

only a quarter of the geometry was modeled. The simplification was possible due to the symmetry of the geometry by applying appropriate boundary conditions.

RESULTS AND DISCUSSION

In Vivo Experiments

To prove the efficacy of electroporation for gene delivery in skin and to localize the expression of a gene in skin after intradermal injection of plasmid, followed by electroporation, a plasmid coding for GFP was used as a reporter gene. To assess the expression, we used a confocal microscope. The results in Fig. 1 show some autofluorescence of hair follicles in the control group where no electroporation was used (Fig. 1a). However, when applying electric pulses after intradermal injection of the plasmid, the expression of GFP was greatly enhanced (Fig. 1b). The location of GFP expression shows that, even by applying electric pulses through external plate electrodes, we successfully breached the highly resistive stratum corneum thus permeabilizing deeper layers of skin (dermis and epidermis).

Geometry of the Numerical Model

In order to get a theoretical insight into the process of *in vivo* electropermeabilization of skin, we made a numerical model of a skin fold, making the geometry as close to the *in vivo* experimental tissue-electrode setup as possible. Four layers of skin were modeled: stratum corneum, epidermis, dermis, and the subcutaneous layer (fat and connective tissue). The electric pulses were applied on the skin with plate electrodes pressed against the skin and were modeled as a boundary condition. The distance between the elec-

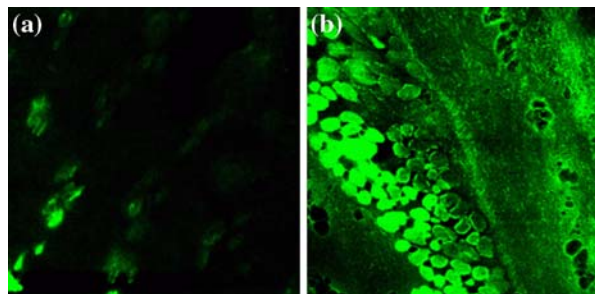


FIGURE 1. GFP expression in skin after intradermal (ID) injection of 50 μg of a plasmid coding for GFP; (a) no electroporation—glowing green areas denote autofluorescence of hair follicles; (b) ID injection + electroporation (400 V 100 μs plus 56 V 400 ms)—GFP expression (shown in green) is enhanced significantly.

trodes was 4 mm and the area in contact with skin was 1 cm^2 (the same as during the *in vivo* experiments). However, to account for the presence of the conductive gel used in experiments in order to assure good contact between the skin and the electrodes, the voltage boundary condition was set somewhat beyond the size of the electrodes. The geometry of our numerical model is shown in Fig. 2. By taking advantage of its symmetry, only a quarter of the whole geometry can be modeled as to avoid numerical problems due to the complexity of the model and computer memory limitations. The cutting planes through which the skin fold was cut into quarters, are shown in Fig. 2a. Boundary conditions on the section planes cut through the middle of the geometry had to be set as shown in Fig. 2b. The thickness of the stratum corneum in the model was set larger than in real skin (around 6 times). Namely, due to the large differences in layer thicknesses, numerical problems can occur that render the calculation impossible. To make up for the stratum corneum being modeled thicker than it is, the conductivity of this very resistive layer was also set higher (6 times). As the experiments showed, the epidermis and the dermis were transfected, indicating that the electric field was high enough in those layers, due to the rise in electrical conductivity of the stratum corneum. Therefore, our numerical model was made nonlinear, the electric field distribution (the model output) depending on the changes in the electrical conductivity of the tissues involved (model input parameters).

Parameters of the Numerical Model

With the model presented we explained the nonlinear process of skin electropermeabilization from the aspect of bulk conductivity changes. Other processes, such as the resealing process during and after pulsing, or the electrophoretic aspect of the electric pulsing were not modeled.

During the finite model analysis, tissue conductivities were changed according to the electric field distribution throughout the model. The process of tissue electropermeabilization was thus modeled in discrete time steps. In each step, the current solution was used to look for the areas where the electric field was above the pre-defined threshold. The conductivity of those areas was changed (increased) and the next step of the modeled electropermeabilization process was computed. This process was repeated until the electric field distribution reached its steady state. That is, when there were no more areas in which the electric field was above the predefined threshold. Also, once the conductivity was increased in a given area, it could not be changed back to its lower value in the following steps, even if the electric field strength should drop below the

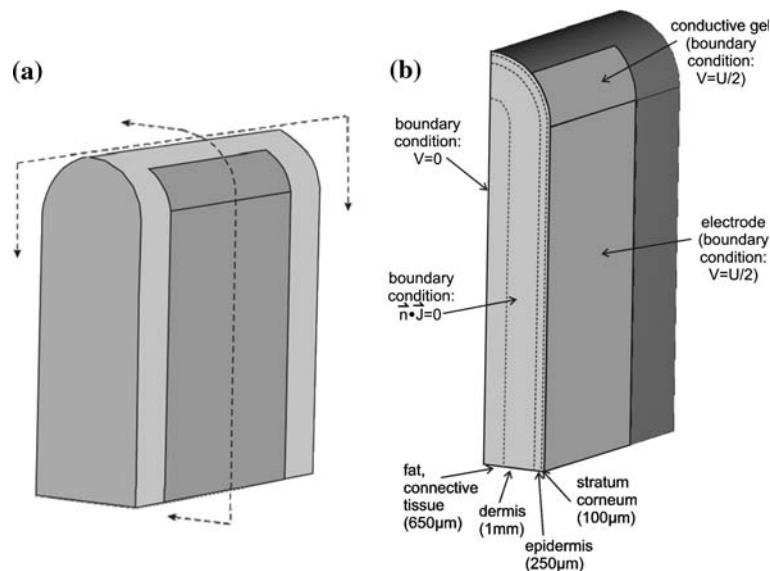


FIGURE 2. (a) A drawing of the whole skin fold, showing the directions in which it was cut in order to get only one quarter of the geometry. (b) Geometry of the skin fold finite element model made in COMSOL. Only a quarter of the skin fold was modeled to avoid numerical problems and save computer time. Boundary conditions were therefore set as shown.

threshold due to changed conductivities. We got the electrical conductivity values and their changes during electroporation from literature and experiments, as well as the electric field values above which tissues are permeabilized.^{4-7,15-18,25,26} However, getting these values was a difficult task, due to the lack of measurements in this field.

Exactly how tissue conductivities (σ) change with electric field (E) is another unknown of tissue electropermeabilization. The simplest of the dependences is the step function, where, once the electric field threshold is reached, the conductivity changes from its low to its high value. However, a kind of a gradual increase of the conductivities seems more “natural.” Namely, due to the non-uniformity of the cell size and shape in the tissue, not all the cells are permeabilized at the same time once the threshold electric field is reached. In our model, the conductivities were increased from their low to their high values in four steps. The conductivity steps for all the skin layers followed an exponential dependence between 60,000 and 140,000 V/m of the electric field strength. For illustration, Fig. 3 shows the $\sigma(E)$ dependence used to model the electropermeabilization of the dermis and the epidermis (excluding its outermost layer, the stratum corneum). The dependences used for the stratum corneum and the subcutaneous layer are not shown. Conductivity increases of all skin layers modeled are summarized in Table 1. Although the dermis and the epidermis were modeled as separate layers, the same conductivity was assigned to both, due to the lack of impedance data on different skin layers.

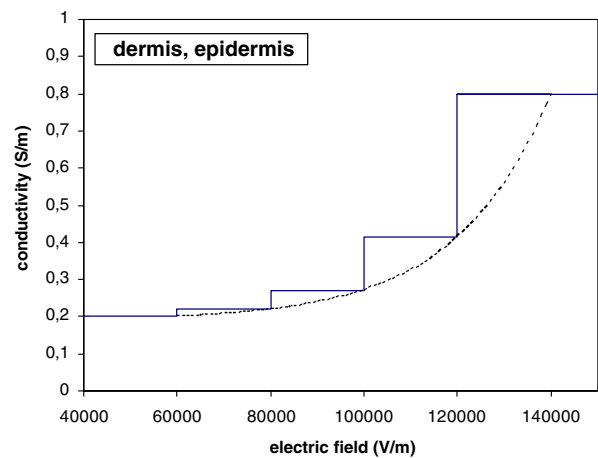


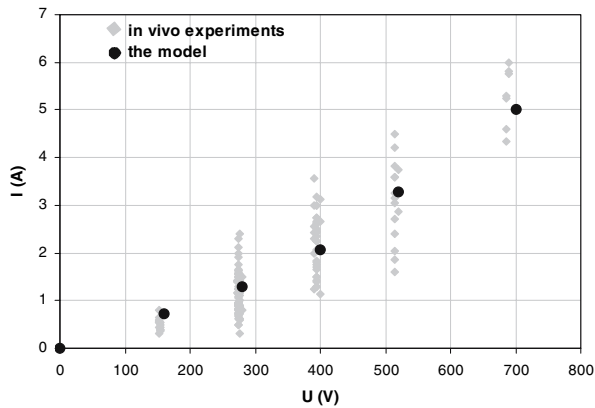
FIGURE 3. Four steps of the dermis and the epidermis (stratum corneum excluded) conductivity increase. The dotted line shows the exponential function used as a basis for the conductivity increase.

In Vivo Experiments—Numerical Model Comparison

During our *in vivo* experiments we tested different amplitudes of the permeabilizing electric pulse. Five different voltage amplitudes were used to permeabilize the skin: 160, 280, 400, 520, and 700 V. During the pulse, the voltage between the electrodes and the current through the skin fold were measured by the Cliniporator and stored on computer. The finite element model of skin electropermeabilization was solved at all five voltages used and the reaction currents obtained from the model were compared to our experimental data. Figure 4 shows the currents

TABLE 1. Conductivity values used in discrete model of the electropermeabilization process in skin.

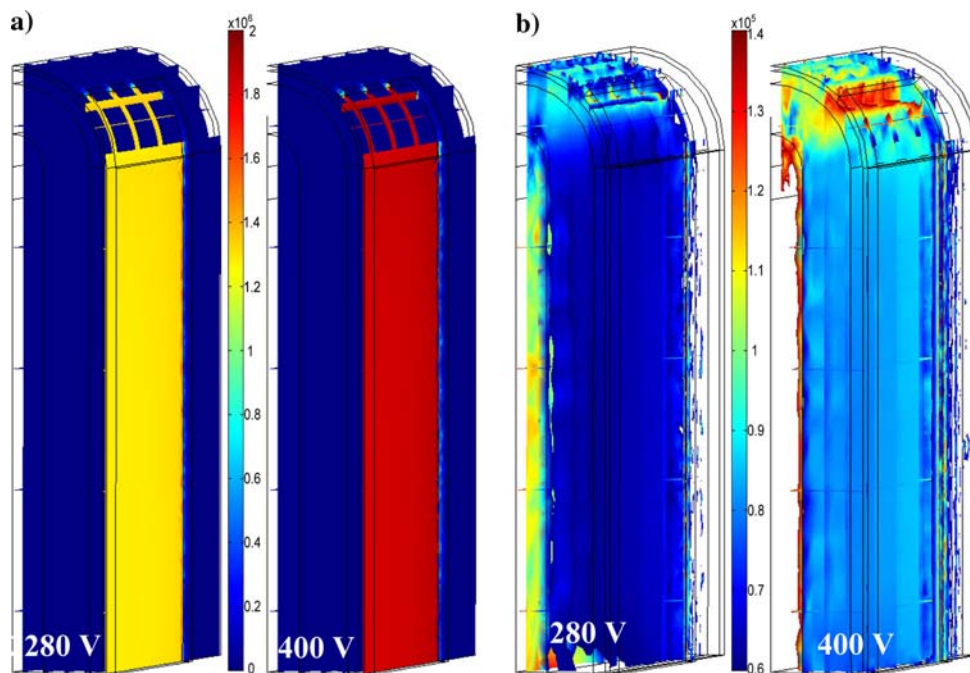
Tissue	$\sigma_{(E < 600 \text{ V/cm})}$ (S/m)	$\sigma_{(600 < E < 800 \text{ V/cm})}$ (S/m)	$\sigma_{(800 < E < 1000 \text{ V/cm})}$ (S/m)	$\sigma_{(1000 < E < 1200 \text{ V/cm})}$ (S/m)	$\sigma_{(E > 1200 \text{ V/cm})}$ (S/m)
Subcutaneous layer	0.05	0.055	0.068	0.103	0.2
Dermis, epidermis	0.2	0.22	0.27	0.41	0.8
Stratum corneum	0.0005	0.0165	0.06	0.178	0.5

**FIGURE 4. Currents measured during the pulse, compared to the currents given by the model, with respect to applied voltages.**

computed by the model compared to the currents measured *in vivo* during the pulse. A good agreement can be observed. Further, the current/voltage depen-

dence given by our model exerts the same nonlinearity as observed from the *in vivo* data, suggesting that the approach we used to describe the process explains well the nonlinear nature of skin electropermeabilization.

Electric field distributions of the skin fold, represented with slice plots in 3D for the applied voltages 280 V and 400 V (the voltages resulting in a successful gene transfection *in vivo*), are presented in Fig. 5. The figures show only one quarter of the geometry, as only a quarter of the skin fold was modeled, taking advantage of the geometrical symmetry. Figure 5a shows the electric field distributions at the beginning of the process, when all the tissues still have their initial conductivities. For both pulse amplitudes, 280 V and 400 V, we can observe a very high electric field in the stratum corneum, while the electric field in deeper layers is still below the permeabilization threshold. Further, the electric field distributions at the end of the electropermeabilization process at 280 V and 400 V are shown in Fig. 5b. The figures show the area between the electric field strength of 600–1400 V/cm,

**FIGURE 5. 3D slice plots of the electric field distributions in the skin fold for the applied voltages of 280 V and 400 V (a) at the beginning of the process when all the tissues still have their initial conductivities; (b) in permeabilized tissue, at the end of the electropermeabilization process. The electric field is shown in volts per meter.**

that is, in the range where the conductivity increase was predicted in the model (blue to red colors). In the non-colored areas the electric field was either below the 600 V/cm (the areas further away from the electrodes), or above 1400 V/cm (low conductive subcutaneous tissue and the topmost part of the skin fold, near areas shown in red).

Dividing the applied voltage with the distance between the electrodes (4 mm), we get the approximate electric field between the plates, which, in the case of 160 V, results in 400 V/cm; 280 V corresponds to 700 V/cm, and so on. According to literature,^{13,23} the approximate threshold for skin electroporation is somewhere above 400 V/cm. The electric field distributions in Fig. 5 suggest that most of the dermis and the epidermis, as predicted by our model, is subjected to electric field above that value. Here we need to be aware that the region of our interest is the topmost part of the skin fold, where, during the *in vivo* experiments, the plasmid was injected intradermally. In fact, the voltage amplitudes of 280 V and 400 V result in a successful gene expression in skin, which seems to be confirmed by the model. *In vivo* experiments showed a lower expression when 160 V was used, which is in agreement with the model, showing too low an electric field in the dermis and the epidermis at 160 V (data not shown). Further, when using higher voltages (520 V or 700 V), the *in vivo* gene expression was lower due to the irreversible membrane permeabilization hence lower cell viability caused by high electric fields. Indeed, the high electric field values given by the model for those voltages suggest an irreversible tissue permeabilization (data not shown).

CONCLUSION

We studied the effectiveness of electroporation for DNA electrotransfer in skin. During *in vivo* experiments, a plasmid coding for GFP was used to localize gene expression in the skin after intradermal injection of the plasmid, followed by electroporation. The expression was assessed with a confocal microscope. Indeed, a significantly higher gene expression was observed when electric pulses were used after the intradermal injection of the plasmid. Furthermore, the location of GFP expression shows that we successfully permeabilized deeper layers of skin (dermis and epidermis). Theoretically, the ratios of the conductivities of the skin layers suggest that the highest voltage drop rests across the stratum corneum, while the electric field in the layers targeted for gene transfection (the dermis and the viable epidermis) is too low for a successful permeabilization (see Fig. 5a). However, due to the nonlinear nature of tissue electroporation,

electric pulses delivered to skin through external plate electrodes breach the highly resistive stratum corneum thus permeabilizing the layers underneath. Namely, electrical conductivities of tissues subjected to electric pulses increase. As a result, the electric field “penetrates” deeper into the skin and permeabilizes target cells (see Fig. 5b). The nonlinear nature of the process was suggested by the current/voltage data measured during the *in vivo* experiments. Increase in pulse amplitude leads to higher reaction currents and electric field in the tissue, however, the increase is not linear. Our numerical model describes this nonlinear process in discrete time steps, using the finite element method. Other processes, such as the resealing process during and after pulsing, or the electrophoretic aspect of the electric pulsing, were not modeled. Also, some simplifications of the geometry were necessary due to its complexity. Electroporation of the skin fold was modeled as an irreversible phase transition problem. The electric field distribution was computed in discrete time steps that represent stages of conductivity changes in tissues during electroporation. The output of the model was compared to the current and the voltage measured during experiments and a good agreement was obtained (Fig. 4). Also, the current/voltage dependence given by our model exerts the same nonlinearity as observed *in vivo*. Further, the voltage amplitudes suggested by the model to cause a successful electroporation coincide well with our *in vivo* results and are in the range of those reported by other authors.

The accuracy of a numerical model depends on many factors. First, the geometry of the model needs to be as close as possible to the *in vivo* geometry. Second, the parameters such as conductivities of permeabilized and non-permeabilized tissue and electroporation thresholds all have an effect on the output of the model. However, data on virtually all these parameters, except the conductivities before the electroporation, are very scarce in the literature, sometimes non-existent. Namely, the subject of tissue conductivity changes due to electroporation described in this paper is still a rather unexplored area. In addition, due to different measuring circumstances, measuring techniques and animal species used by different researchers, large discrepancies can be found in the reported data on tissue conductivities. Therefore, certain inaccuracies could not be avoided in the numerical model presented. In our future work we intend to establish the level of confidence in such a model with a parameterization study. Further, we plan to improve the model by gathering more data on conductivity changes during skin electroporation. Nevertheless, the model presented in this paper serves as a proof of principle of the tissue electroporation.

meabilization propagation beyond the initial conditions dictated by the tissue initial conductivities.

ACKNOWLEDGMENTS

This research was supported by the European Commission under the 5th framework under the grant Cliniporator QLK-1999-00484 and the Slovenian Research Agency.

REFERENCES

- ¹Chizmadzhev, Y. A., A. V. Indenbom, P. I. Kuzmin, S. V. Galichenko, J. C. Weaver, and R. O. Potts. Electrical properties of skin at moderate voltages: contribution of appendageal macropores. *Biophys. J.* 74:843–856, 1998.
- ²Drabick, J. J., J. Glasspool-Malone, A. King, and R. W. Malone. Cutaneous transfection and immune responses to intradermal nucleic acid vaccination are significantly enhanced by in vivo electroporation. *Mol. Ther.* 3(2):249–255, 2001.
- ³Ferber, D. Gene therapy: safer and virus-free? *Science* 294:1638–1642, 2001.
- ⁴Gabriel, C., S. Gabriel, and E. Corthout. The dielectric properties of biological tissues: I. Literature survey. *Phys. Med. Biol.* 41:2231–2249, 1996.
- ⁵Gabriel, S., R. W. Lau, and C. Gabriel. The dielectric properties of biological tissues: II. Measurements in the frequency range 10 Hz to 20 GHz. *Phys. Med. Biol.* 41:2251–2269, 1996.
- ⁶Gallo, S. A., A. R. Oseroff, P. G. Johnson, and S. W. Hui. Characterization of electric-pulse-induced permeabilization of porcine skin using surface electrodes. *Biophys. J.* 72:2805–2811, 1997.
- ⁷Jadoul, A., J. Bouwstra, and V. Pr eat. Effects of iontophoresis and electroporation on the stratum corneum; Review of the biophysical studies. *Adv. Drug Deliv. Rev.* 35:89–105, 1999.
- ⁸Mehier-Humbert, S., and R. H. Guy. Physical methods for gene transfer: improving the kinetic of gene delivery into cells. *Adv. Drug Del. Rev.* 57(5):733–753, 2005.
- ⁹Menon, G. K. New insights into skin structure: scratching the surface. *Adv. Drug Deliv. Rev.* 54(Suppl.1):S3–S17, 2002.
- ¹⁰Mir, L. M. Therapeutic perspectives of in vivo cell electroporation. Review article. *Bioelectrochemistry* 53:1–10, 2000.
- ¹¹Pavlin, M., and D. Miklav ci c. Effective conductivity of a suspension of permeabilized cells: a theoretical analysis. *Biophys. J.* 85:719–729, 2003.
- ¹²Pavlin, M., N. Pav selj, and D. Miklav ci c. Dependence of induced transmembrane potential on cell density, arrangement and cell position inside a cell system. *IEEE Trans. Biomed. Eng.* 49(6):605–612, 2002.
- ¹³Pav selj, N., Z. Bregar, D. Cukjati, D. Batiuskaite, L. M. Mir, and D. Miklav ci c. The course of tissue permeabilization studied on a mathematical model of a subcutaneous tumor in small animals. *IEEE Trans. Biomed. Eng.* 52(8):1373–1381, 2005.
- ¹⁴Pav selj, N., and V. Pr eat. DNA electrotransfer into the skin using a combination of one high- and one low-voltage pulse. *J. Cont. Rel.* 106:407–415, 2005.
- ¹⁵Pliquett, U. Mechanistic studies of molecular transdermal transport due to skin electroporation. *Adv. Drug. Deliv. Rev.* 35:41–60, 1999.
- ¹⁶Pliquett, U., R. Langer, and J. C. Weaver. Changes in the passive electrical properties of human stratum corneum due to electroporation. *Biochim. Biophys. Acta* 1239:111–121, 1995.
- ¹⁷Pliquett, U., and J. C. Weaver. Electroporation of human skin: simultaneous measurement of changes in the transport of two fluorescent molecules and in the passive electrical properties. *Bioelectrochem. Bioenerg.* 39:1–12, 1996.
- ¹⁸Prausnitz, M. R., V. G. Bose, R. Langer, and J. C. Weaver. Electroporation of mammalian skin: a mechanism to enhance transdermal drug delivery. *Proc. Natl. Acad. Sci. USA* 90:10504–10508, 1993.
- ¹⁹Prud'homme, G. J., Y. Glinka, A. S. Khan, and R. Draghia-Akli. Electroporation-enhanced nonviral gene transfer for the prevention of treatment of immunological, endocrine and neoplastic diseases. *Curr. Gene Ther.* 6:243–273, 2006.
- ²⁰Susil, R., D.  semrov, and D. Miklav ci c. Electric field – induced transmembrane potential depends on cell density and organization. *Electro Magnetobiol.* 17(3):391–399, 1998.
- ²¹ sel, D., D. Cukjati, D. Batiuskaite, T. Slivnik, L. M. Mir, and D. Miklav ci c. Sequential finite element model of tissue electroporation. *IEEE Trans. Biomed. Eng.* 52:816–827, 2005.
- ²²Vali c, B., M. Golzio, M. Pavlin, A. Schatz, C. Faurie, B. Gabriel, J. Teissi c, M. P. Rols, and D. Miklav ci c. Effect of electric field induced transmembrane potential on spheroidal cells: theory and experiment. *Eur. Biophys. J.* 32:519–528, 2003.
- ²³Weaver, J. C., T. E. Vaughan, and Y. Chizmadzhev. Theory of electrical creation of aqueous pathways across skin transport barriers. *Adv. Drug Del. Rev.* 35:21–39, 1999.
- ²⁴Wolf, H., M. P. Rols, E. Boldt, E. Neumann, and J. Teissi c. Control by pulse parameters of electric field-mediated gene transfer in mammalian cells. *Biophys. J.* 66:524–531, 1994.
- ²⁵Yamamoto, T., and Y. Yamamoto. Electrical properties of the epidermal stratum corneum. *Med. Biol. Eng.* 14(2):151–158, 1976.
- ²⁶Yamamoto, T., and Y. Yamamoto. Dielectric constant and resistivity of epidermal stratum corneum. *Med. Biol. Eng.* 14(5):494–500, 1976.
- ²⁷Zhang, L., G. Widera, and D. Rabussay. Enhancement of the effectiveness of electroporation-augmented cutaneous DNA vaccination by a particulate adjuvant. *Bioelectrochemistry* 63(1–2):369–373, 2004.